Available online at www.sciencedirect.com
ScienceDirect
Electrochimica Acta 52 (2007) 6106–6117
ELECTROCHIMICA Acta
www.elsevier.com/locate/electacta

Electrochemical study of binary and ternary copper complexes in ammonia-chloride medium

Jorge Vazquez-Arenas, Isabel Lazaro, Roel Cruz *

Facultad de Ingeniería-Instituto de Metalurgia, Universidad Autónoma de San Luis Potosí, Av. Sierra Leona No. 550, Lomas 2a Sección, 78210 San Luis Potosí, S.L.P., Mexico

Received 24 December 2006; received in revised form 5 March 2007; accepted 22 March 2007
Available online 25 March 2007

Abstract

Electrochemical and spectroscopic analyses (UV–vis and XRD) have been applied to evaluate the speciation of copper in ammonia-chloride solutions. The conditions for these analyses were established through thermodynamic studies that included predominance existence and E_h–pH diagrams. These studies highlighted the importance of copper ternary complexes and showed how the solubility of Cu(I) and Cu(II) increases over a wide range of pH when copper ternary complexes are formed. Hence, it has been elucidated the copper, ammonia and chloride concentrations that makes existence of these so-called copper ternary complexes, possible.

Keywords: Copper complexes; Ammonia; Chloride; Thermodynamic; Voltammetry

1. Introduction

The electrolytic recovery of copper from sulfate solutions is the most common process applied in many hydrometallurgical processes currently in operation, all of this as a result of the general advantages that this medium offers, particularly permitting wire bar grade cathodic deposits [1]. The characteristics of the sulfate medium have in fact limited the use of other media in leaching processes because of considerations of having to convert anyway to sulfate, in order to comply with the requirements of the electrolytic process [2]. Such is the case of the chloride media that is reported to improve the kinetics of dissolution but has the drawback of being a corrosive environment [3]. To overcome the corrosive characteristics of the chloride medium, some authors have proposed the combination of this medium with ammonia, which inhibits the formation of chlorine gas and is also a much stronger complexing agent [4–6]. To our knowledge two hydrometallurgical based ammonia chloride (NH_4Cl) processes have been applied successfully at industrial levels, the CENIM-LNETI process for base metals and the Ezinex® process for zinc recovery [5,6].

The characteristics described for the ammonium chloride system such as improving leaching and also the possibility of working at a pH value that provokes that any iron and other minor elements considered as impurities remain in the residue after leaching [5], have prompted studies that have addressed thermodynamic and electrochemical aspects. Most of these studies described Cu(II) and/or Cu(I) complexation and solubility aspects [7–9]. Early work by Limpo et al. focused mainly on effects of experimental conditions on the solubility of Cu(II) [7]. These authors found that the solubility of Cu(II) in this medium is restricted by either the solubility of $Cu(NH_3)_2Cl_2$ or $Cu(OH)_{1.5}Cl_{0.5}$, the predominance of both precipitates dependent on chloride concentration. They observed that in the range of 5–9m, the Cu(II) diammine chloride is generally the solid phase whose solubility regulates that of Cu(II); the hydroxychloride becomes the most insoluble solid compound and hence the substance which restricts the solubility of the Cu(II), only at the lowest test levels of chlorides and when the ratio of $[NH_3]$ and [Cu] is less than 2. Hence, in that work they showed the need of including the formation of ternary complexes of copper ammonia-chloride with the general formula $CuCl_x(NH_3)_{4-x}$, in order to interpret experimental solubility data and get a better fit with the predicted values obtained with theoretical models. Likewise, later work by Solis et al., highlighted the importance of Cu(I) ternary complexes and provided experimental

* Corresponding author. Tel.: +52 444 825 43 26; fax: +52 444 825 43 26.
E-mail address: rcuz@uaslp.mx (R. Cruz).

0013-4686/$ – see front matter © 2007 Elsevier Ltd. All rights reserved.
doi:10.1016/j.electacta.2007.03.062

thermodynamic data for the Cu(I)–ammonia-chloride system [8].

Nila and González [9] experimentally confirmed that Cu(II) solubility was limited by formation of the hydroxychloride precipitate ($Cu(OH)_{1.5}Cl_{0.5}$). These authors did not report Cu(II) solubility limitations by formation of $Cu(NH_3)_2Cl_2$ as did Limpo et al. [7], but this could be attributed to the fact that the concentration of chloride they used was never higher than 1 M.

With the exception of some reports [9–11], most of the research studies have been oriented towards leaching conditions and in fact recent works are more concerned with the application of the Cu(II) tetrammine complex as an oxidizing agent for thiosulfate leaching of gold [12,13].

The dissolution and stabilization of copper in hydrometallurgical operations such as leaching and electrowinning require very high concentrations of chloride and ammonia [5,6]. In spite of this the evaluation of the redox system Cu(I)/Cu(II) under such conditions has been scarcely studied, and even the importance of the binary and ternary complexes has been overlooked in electrochemical studies. A better understanding of the characteristics of theses systems could allow an improved assessment of this medium.

Therefore, the present study aims to further highlight the existence of binary and ternary complexes for both Cu(I) and Cu(II) in ammonia-chloride medium by means of electrochemical characterization of Cu(I)/Cu(II) redox couples. Likewise spectroscopic techniques (UV, XRD) were used to characterize the predominant soluble and insoluble species under conditions of high chloride and high ammonia concentrations. The experimental approach was based on thermodynamic predictions.

2. Experimental

All solutions employed in this work were prepared using reagents of analytical quality and deionized water (18.2 μΩ cm) obtained by inverse osmosis (Barnstead™). Unless otherwise stated all Cu(II) solutions were prepared using $CuCl_2{\cdot}2H_2O$, NH_4Cl and in some instances NH_4OH. Variation of solutions pH was achieved by adjustment and control with either 4 M NaOH or 10 M H_2SO_4 solutions. Cu(I) solutions were prepared by dissolution of cuprous chloride salt (CuCl) in solution 4 M of NH_4Cl and adjusted to the required pH. To warrant the presence of Cu(I) complexes, hydrazine dihydrochloride was added to the solution as an stabilizer agent. All Cu(I) solutions were prepared with deionized water which had been previously deareated with nitrogen for about 40 min. To prevent oxidation of Cu(I) a nitrogen atmosphere was kept during the period of analysis. Fresh Cu(I) solutions were colorless and it took approximately 2 h for them to turn to colored solutions indicating presence of Cu(II) complexes.

A conventional three-electrode cell was used for electrochemical experiments. A glassy carbon (GC) cylinder was used to construct a disk electrode. The disk electrode was made by embedding the GC cylinder in Teflon, allowing the exposure of only one face with an area of 0.38 cm^2. A graphite rod was employed as counter electrode and a saturated calomel electrode (SCE) as reference electrode, with a potential of 241 mV versus the standard hydrogen electrode (SHE). For convenience, all potentials reported here have been converted to the SHE scale. Before making any electrochemical measurements, the surface of the disk was prepared by being ground on fine silicon carbide paper (grade 600 and 2000), polishing to a mirror finish with 0.05 μm alumina paste followed by ultrasonic cleaning. The electrochemical measurements were carried out using an AUTOLAB™ model PGSTAT 30 potenstiotat–galvanostat coupled to a personal computer.

UV–vis spectrophotometric analysis of solutions was carried using a Lambda 35 Perkin-Elmer™. Solid samples were characterized by X-ray diffraction (XRD) analysis using a Phillips Rigaku™ DMAX 2200 diffractometer.

3. Results and discussion

3.1. Thermodynamic study

In order to establish different thermodynamic aspects of the $Cu–NH_4Cl–NH_3–H_2O$ system, it is important to have a wide knowledge of the solution chemistry of the different species involved. Thus, in this study graphical methods such as species distribution and predominance area (including E_h–pH) diagrams were constructed to illustrate the various possible equilibrium reactions for copper in an ammonia-chloride media. The construction of these thermodynamic diagrams was based on free energy minimization algorithms reported by Eriksson [14], and used by the Chemical Equilibrium Software MEDUSA® [15]. The equilibrium constants for complex formation were taken from the critically selected stability constants published by the National Institute of Standards and Technology [16] and others from the literature (Tables 1–3) [7,8,17–20]. Furthermore, these data were complemented with the HYDRA program database [15].

For many of the constants there is a wide variety of values and conditions under which each was obtained, thus in a similar way as that proposed by Limpo et al. [7], a path was followed in which the criteria of selection of constants was based on the value of ionic strength at which they were obtained. Although, it is acknowledged that aqueous electrolyte solutions with

Table 1
Thermodynamic data for chlorocomplexes, used in the construction of the Cu(I)/Cu(II)–NH_4Cl–NH_3–H_2O diagrams, at 298 K

Complex	log β	Ionic strength	Reference
$Cu^+ + Cl^- = CuCl_{(ac)}$	2.70	5	[17]
$Cu^+ + 2Cl^- = CuCl_2^-$	6	5	[17]
$Cu^+ + 3Cl^- = CuCl_3^{2-}$	5.99	High	[19]
$2Cu^+ + 4Cl^- = Cu_2Cl_4^{2-}$	10.57	–	[14]
$Cu^+ + Cl^- = CuCl_{(s)}$	7.38	–	[14]
$Cu^{2+} + Cl^- = CuCl^+$	0.60	5	[16]
$Cu^{2+} + 2Cl^- = CuCl_{2(ac)}$	0.67	5	[16]
$Cu^{2+} + 3Cl^- = CuCl_3^-$	0.30	5	[16]
$Cu^{2+} + 4Cl^- = CuCl_4^{2-}$	−0.64	5	[16]
$Cu^{2+} + 1.5OH^- + 0.5Cl^- = CuOH_{1.5}Cl_{0.5(s)}$	17.3	0	[15]

Table 2
Thermodynamic data for hydroxo-complexes, used in the construction of the Cu(I)/Cu(II)–NH_4Cl–NH_3–H_2O diagrams, at 298 K [15]

Complex	log β	Ionic strength a
$Cu^+ + OH^- = 0.5Cu_2O_{(s)} + 0.5H_2O$	14.7	0
$Cu^{2+} + OH^- = CuOH^+$	6.8 (±2)	3
$Cu^{2+} + 2OH^- = CuOH_{2(ac)}$	11.2 (±4)	0.7
$Cu^{2+} + 3OH^- = CuOH_3^-$	14.5	1
$Cu^{2+} + 4OH^- = CuOH_4^{2-}$	15.6	1
$Cu^{2+} + 2OH^- = CuOH_{2(s)}$	18.9	1
$Cu^{2+} + 2OH^- = CuO_{(s)} + H_2O$	19.51	0.7

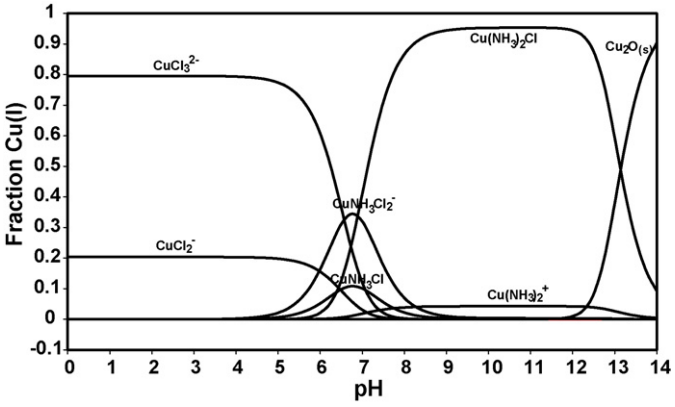

Fig. 1. Species distribution diagram for copper (I) complexes in a solution containing a total concentration of 0.2 M Cu(I) and 4 M NH_4Cl.

concentration of ions greater than about 1×10^{-6} M do not behave ideally, it is considered a practical way for treatment of real hydrometallurgical systems, as they generally involve solutions highly concentrated (such as the ones in the present study), and especially those used in the electrolytic stage.

3.1.1. Species distribution diagram for Cu(I)–NH_4Cl–NH_3–H_2O system

The species distribution diagram for the Cu(I)–NH_4Cl–NH_3–H_2O system is illustrated in Fig. 1. This diagram shows the fraction of species present as a function of pH. Given the predominance of NH_4^+ at pH values below 6, no copper ammine complexes are observed in this pH zone and thus the chloride complexes account for most of the total Cu(I) concentration. As shown in Fig. 1, in this pH region the predominant species is $CuCl_3^{2-}$. As pH increases, $Cu(NH_3)_2Cl$ becomes the predominant species producing the highest solubility of Cu(I) for one individual species, since its fraction is around 0.95 at pH's values within 8.5–12.5. The solid phases evaluated were the $CuCl_{(s)}$ and $Cu_2O_{(s)}$, as it has been reported in the literature [9,21–23]. However, for the conditions at which the diagram was constructed, the $Cu_2O_{(s)}$, exhibits the highest stability. The solid phase was determined for pH > 12.5.

3.1.2. Predominance diagrams for Cu(I)

To determine the formation of soluble and solid phases under different conditions for the Cu(I)–NH_4Cl–NH_3–H_2O system, independent predominance diagrams were constructed as a function of Cu(I), NH_3 and Cl^- concentrations versus pH.

In all diagrams, the doted lines indicate the conditions to be evaluated in this study, which are those used for distribution diagram construction (Fig. 1). The diagrams obtained show the predominance zone of different complexes and solid phases (Fig. 2). Hence, it can be observed that for the acidic zone (pH < 6.57) the trichloride complex ($CuCl_3^{2-}$) predominates as far as the chloride concentration is higher than ~1 M ($pCl^- < 0$). For lower chloride concentrations, the formation of the solid phase $CuCl_{(s)}$ would take place due to the low stability of the $CuCl_2^-$ complex [9,21–23].

For the neutral region, there is an important variation of predominant copper species which is strongly affected by changes in ammonia and chloride concentrations, and that is why we labeled this zone as ligands interchange zone. Hence, as the ammonia concentration increases the predominant complexes change as follows: $CuCl_3^{2-} \rightarrow CuNH_3Cl_2^- \rightarrow Cu(NH_3)_2Cl$. For the conditions to be evaluated in this work, $CuNH_3Cl_2^-$ would be the predominant specie at 6.57 < pH < 6.89. In the neutral-alkaline zone, the $Cu(NH_3)_2Cl$ exhibits a wide

Table 3
Thermodynamic data for amino-complexes, used in the construction of the Cu(I)/Cu(II)–NH_4Cl–NH_3–H_2O 25 °C diagrams, at 298 K

Complex	log β	Ionic strength	Reference
$NH_3 + H^+ = NH_4^+$	9.4	1	[17]
$Cu^+ + NH_3 = CuNH_3^+$	5.93	2	[15]
$Cu^+ + 2NH_3 = Cu(NH_3)_2^+$	10.58	2	[15]
$Cu^+ + NH_3 + Cl^- = CuNH_3Cl_{(ac)}$	8.92	1	[8]
$Cu^+ + NH_3 + 2Cl^- = CuNH_3Cl_2^-$	8.82	1	[8]
$Cu^+ + 2NH_3 + Cl^- = Cu(NH_3)_2Cl_{(ac)}$	11.33	1	[8]
$Cu^{2+} + NH_3 = CuNH_3^{2+}$	4.2 (±2)	2	[15]
$Cu^{2+} + 2NH_3 = Cu(NH_3)_2^{2+}$	7.75 (±5)	2	[15]
$Cu^{2+} + 3NH_3 = Cu(NH_3)_3^{2+}$	10.6 (±1)	2	[15]
$Cu^{2+} + 4NH_3 = Cu(NH_3)_4^{2+}$	12.9 (±1)	2	[15]
$Cu^{2+} + 5NH_3 = Cu(NH_3)_5^{2+}$	12.43	2	[17]
$Cu^{2+} + NH_3 + OH^- = CuNH_3OH^+$	14.9	–	[17]
$Cu^{2+} + NH_3 + 3OH^- = CuNH_3(OH)_3^-$	16.3	–	[17]
$Cu^{2+} + 2NH_3 + 2OH^- = Cu(NH_3)_2(OH)_{2(ac)}$	15.7	–	[17]
$Cu^{2+} + NH_3 + 3Cl^- = CuNH_3Cl_3^-$	3.62	5	[7]
$Cu^{2+} + 3NH_3 + Cl^- = Cu(NH_3)_3Cl^+$	11.73	5	[7]

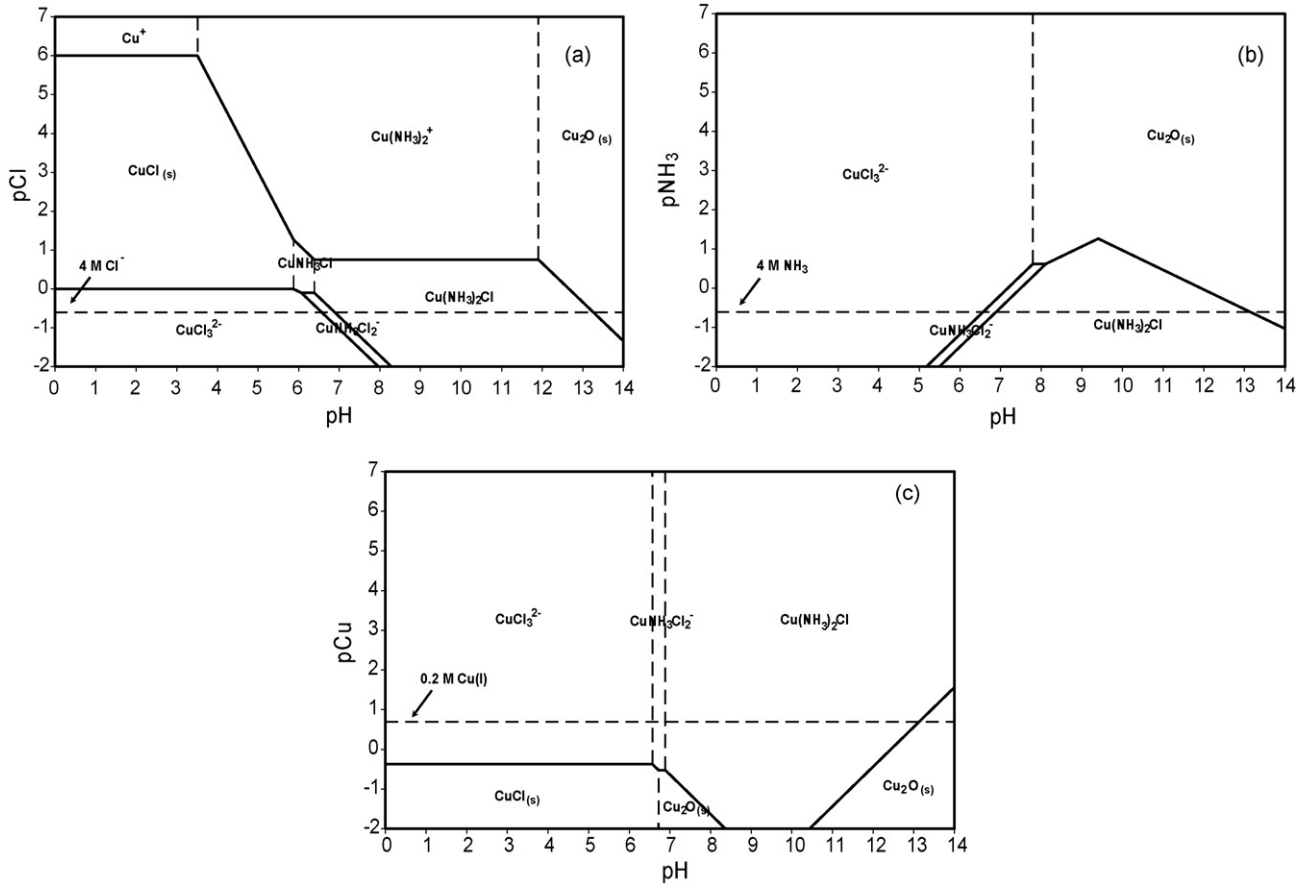

Fig. 2. Predominance area diagrams for Cu(I) constructed as pX (X = [Cu], [NH3], [Cl^-]) functions of pH: (a) pCu, [$NH_4^+ + NH_3$] = 4 M, [Cl^-] = 4 M, (b) $p$$NH_3$, $[Cu]_{total}$ = 0.2 M, [Cl^-] = 4 M and (c) pCl, $[Cu]_{total}$ = 0.2 M, [$NH_4^+ + NH_3$] = 4 M. Dotted lines show the changes produced in the predominant species areas when no ternary complexes are considered.

predominance, which is only limited for the $Cu(NH_3)_2^+$, when chloride concentration decreases below 0.178 M (Fig. 2a) and for $Cu_2O_{(s)}$ for pH > 13.13 (Fig. 2). The formation of Cu_2O(s) is actually promoted by the lack of NH_4^+ that acts as a buffer and removes OH^- ions.

From the diagrams, illustrated in Fig. 2, it is possible to generate lineal diagrams showing the dominant species as a function of pH. Thus, for the system under study – 0.2 M Cu(I) (pCu = 0.698), 4 M NH_3 ($p$$NH_3$ = −0.602) and 4 M Cl^- ($p$$Cl^-$ = −0.602) – the corresponding lineal diagram would be as follows:

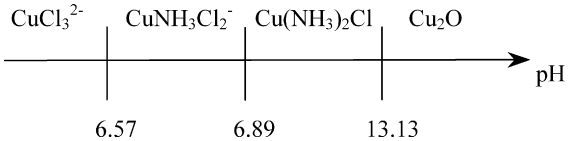

(1)

The above lineal diagram shows four pH regions for the predominant species. This diagram also illustrates in a very simple way the change of ligands towards species of higher stability. The ternary complexes cover a wide stability region due to the combined effect of chloride and ammonia ligands.

3.1.3. Species distribution diagram for Cu(II)–NH_4Cl–NH_3–H_2O

Fig. 3 shows species distribution diagrams for Cu(II) for the same condition of the Cu(I) system. From this diagram it can observed that a lower affinity for chloride complexes is obtained

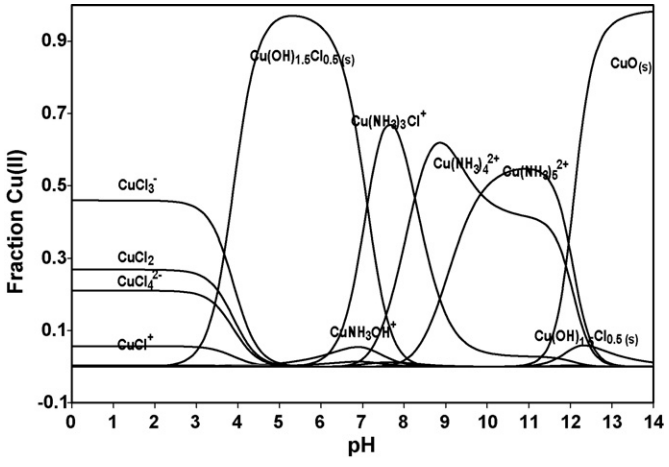

Fig. 3. Species distribution diagram for copper(II) complexes in a solution containing a total concentration of 0.2 M Cu(II) and 4 M NH_4Cl.

for Cu(II) in comparison with the Cu(I) system. The total copper concentration is distributed mainly in three different chloride complexes ($CuCl_3^-$, $CuCl_2$, $CuCl_4^{2-}$) for pH values below ~4. In the region, 4 < pH < 7 a mixed precipitate, $Cu(OH)_{1.5}Cl_{0.5\,(s)}$, would be expected. In agreement with the stability constant of this solid, the copper is practically insoluble in this region, even under conditions where ternary complexes such as $CuNH_3OH^+$ and $Cu(NH_3)_3Cl^+$ could exist. For a pH zone around 7–8.2, the $Cu(NH_3)_3Cl^+$ is the predominant complex. As the pH increases, the amount of NH_3 increases, and this provokes a displacement of the Cl^- ligand out of the Cu(II) coordination sphere. Hence, for pH > 8.2, $Cu(NH_3)_4^{2+}$ is the main complex, meanwhile the $Cu(NH_3)_5^{2+}$ is for pH > 9.4. Finally, at pH > 12.3 $CuO_{(s)}$ formation occurs.

3.1.4. Predominance diagrams for Cu(II)

Similarly to the Cu(I) system, predominance diagrams of Cu(II) species were independently constructed as a function of Cu(II), NH_3 and Cl^- concentrations. Fig. 4 shows that two solid phases are formed, one in the acidic-neutral zone, $Cu(OH)_{1.5}Cl_{0.5(s)}$, and another in the alkaline zone, $CuO_{(s)}$. In the acidic zone pH < 4, the Cu(II) would be soluble under any system condition. Copper aquocomplexes would be generated for chloride concentration lower than 2.51 M (pCl > 0.6). For the conditions here evaluated, the $CuCl_3^-$ is the predominant species, but for pH > 4.13 the formation of $Cu(OH)_{1.5}Cl_{0.5(s)}$ takes place. Earlier publications have reported a coexistence between $Cu(OH)_{1.5}Cl_{0.5(s)}$ and soluble Cu(II) in the form of $Cu(NH_3)_4^{2+}$ at pH values around 7.66 for a total copper concentration of around 0.01 M [9,24]. The incorporation of ternary complexes data in the present thermodynamic study shows that the Cu(II) solubility region widens, and complexes such as $Cu(NH_3)_3Cl^+$ can be formed at pH ~ 6.6 for copper concentrations of 0.2 M. Contrary to what Limpo reported [7], $Cu(NH_3)_2Cl_2$ precipitate was not predicted according to our calculations, even at a chloride/ammonia concentration ratio of 10. This fact is attributed to the low K_{ps} of this precipitate ($10^{-1.7}$). For pH > 8 $Cu(NH_3)_4^{2+}$ and $Cu(NH_3)_5^{2+}$ are formed due to the high ammonia concentration. It is worth noting, that even when Fig. 4a and c indicate that for pH > 9.4 (equilibrium point of $NH_3 - NH_4^+$) the predominance of $Cu(NH_3)_5^{2+}$ is expected, results of Fig. 4a indicate that this complex would be in coexistence with $Cu(NH_3)_4^{2+}$ at the conditions here evaluated. This fact is better observed when the $NH_3 + NH_4^+$ concentration decreases below 4 M. Similarly to the Cu(I) system in the alkaline zone, as the hydroxide concentration increases the copper soluble species stability decreases provoking its precipitation, that for this system is as CuO at pH > 12.3.

From the diagrams shown in Fig. 4, the following lineal diagram was constructed for 0.2 M Cu(II) (pCu = 0.698), 4 M NH_3

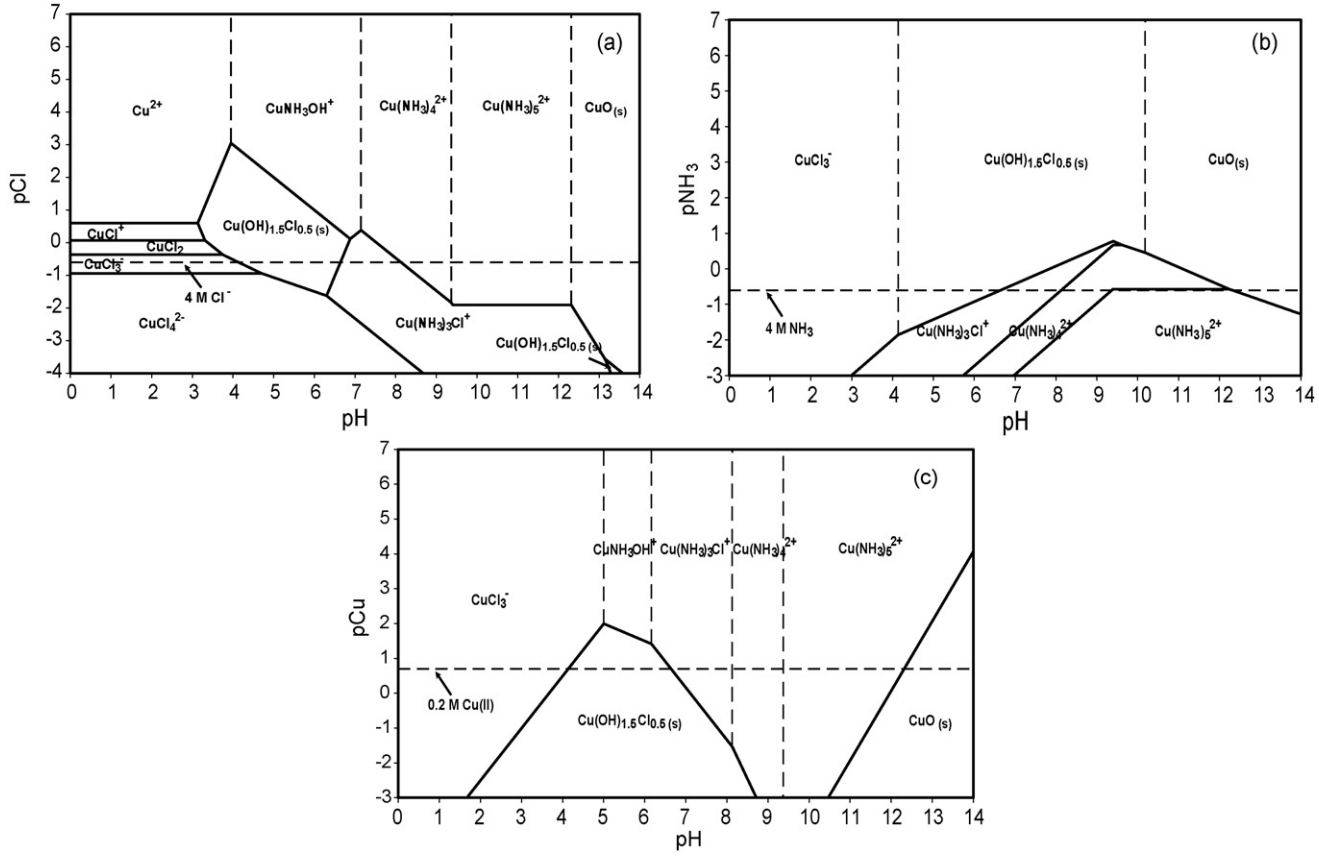

Fig. 4. Predominance area diagrams for Cu(II) constructed as pX's (X = [Cu], [NH_3], [Cl^-]) functions of pH: (a) pCu, [$NH_4^+ + NH_3$] = 4 M, [Cl^-] = 4 M, (b) $p$$NH_3$, $[Cu]_{total}$ = 0.2 M, [Cl^-] = 4 M and (c) pCl, $[Cu]_{total}$ = 0.2 M, [$NH_4^+ + NH_3$] = 4 M. Dotted lines show the changes produced in the predominant species areas when no ternary complexes are considered.

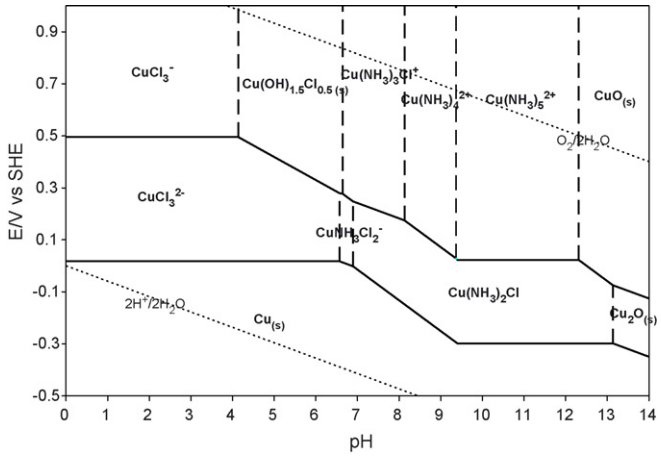

Fig. 5. E_h–pH diagram for Cu–NH_3–Cl–H_2O system at 25 °C. [Cu] = 0.2 M, [Cl^-] = 4 M, [$NH_4^+ + NH_3$] = 4 M.

($pNH_3 = -0.602$) and 4 M Cl^- ($pCl^- = -0.602$):

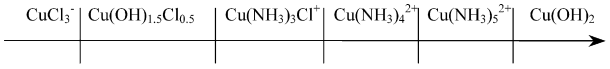

(2)

This diagram illustrates the three solubility zones for Cu(II):chlorocomplexes, ternary complexes and ammine complexes. The chlorocomplexes dominate the acid zone, with the $CuCl_3^-$ as the most stable of all. The zone of ternary complexes, particularly $Cu(NH_3)_3Cl^+$, represents a very interesting option given the advantages of operating processes within the neutral-basic pH region [7]. Finally, the ammine complexes zone involves $Cu(NH_3)_4^{2+}$ and $Cu(NH_3)_5^{2+}$ which although highly stable predominate in a pH region unsuitable because of continuous loss of ammonia.

3.1.5. E_h–pH diagram for Cu(II)–Cu(I)–NH_4Cl–NH_3 system

From the data above discussed, an E_h–pH diagram was constructed for the conditions to be evaluated in this work (Fig. 5). All the equilibriums involving redox reactions were evaluated using the Nernst equation. In a similar way to that illustrated by the lineal diagrams, the different predominant zones are shown as a function of pH as well as the effect of potential on ligand coordination changes for both Cu(I) and Cu(II) ions.

As it was shown above, for the experimental conditions here studied, there are several complexes involved for both Cu(II) and Cu(I) systems. In fact for the Cu(I) system, the ammine complexes are not formed due to the high stability of the ternary complex $Cu(NH_3)_2Cl$.

The precipitate $Cu(OH)_{1.5}Cl_{0.5(s)}$ limits the solubility of Cu(II) at acid pH and $CuO_{(s)}$ at alkaline pH. While there is no indication of solubility limitation at acid pH for Cu(I) at alkaline pH it is limited because of formation of $Cu_2O_{(s)}$.

It is clear that the potential required to reduce Cu(II) to Cu(I), increases as the pH is raised, due to the higher stability of the ammine complexes. Similarly, the potential required to reduce Cu(I) complexes to Cu(0), is higher as the pH increase, however, it was observed that for the neutral pH (ligands' transfer zone) the total overpotential to reduce Cu(II) species to Cu(0) is the lowest, i.e. ~250 mV for ternary complexes at pH 7, while for chloride and amine complexes, the overpotentials are 430 and 320 mV, respectively.

3.2. Spectroscopic characterization of complexes and solid phases

3.2.1. UV–vis spectrophotometric analysis of complexes

In order to obtain experimental data to support the results of the thermodynamic study, solutions of Cu(I) and Cu(II) were analyzed by UV–vis spectrophotometry. The analyses were carried out with copper solutions prepared under specific experimental conditions that favor the formation of the predominant copper soluble species reported in the E_h–pH diagram (Fig. 5; Table 4).

For comparison purpose, a UV–vis spectrum for a 4 M NH_4Cl solution was included in each graph as a blank that allows to evaluate the existence of the predominant species for each condition. Hence, it was observed than the ammonium and chloride by themselves only show an absorption band for a wavelength in the UV region, around 205 nm. For the Cu(I) system, no absorption was expected for the visible region, given that according to the electronic configuration of Cu(I), it does not generate colored complexes. However, for wavelengths in the UV region an important absorption is observed for this system (Fig. 6a), which is greatly affected by changes in pH. As the pH increases, the absorption band at wavelengths around 280–300 nm decreases. Thus, this absorption is attributed to an electronic transition between Cu(I) and Cl^- ions in $CuCl_3^{2-}$ as it has been reported by others authors [8]. When the pH increases the $Cu(NH_3)_2Cl$ becomes the predominant specie and therefore the absorption band at wavelengths of ca. 280 nm decreases (Fig. 6b). Note that

Table 4
Experimental details and results produced by UV–vis spectrophotometric analyses

Solution	Figure	pH	λ (nm)	Species
4 M NH_4Cl + NaOH	Fig. 7	7.5	205	NH_4Cl
0.02 M Cu(I) + 4 M NH_4Cl	Fig. 7a	3	240, 280	$CuCl_3^{2-}$
0.02 M Cu(I) + 4 M NH_4Cl	Fig. 7b	9.3	240	$Cu(NH_3)_2Cl$
0.02 M Cu(II) + 4 M NH_4Cl	Fig. 7c	3.0	240, ~300, 873	$CuCl_3^-$
0.02 M Cu(II) + 4 M NH_4Cl	Fig. 7d	7.4	~240, 660	$Cu(NH_3)_3Cl^+$
0.02 M Cu(II) + 4 M NH_4Cl	Fig. 7d	8.7	~240, 605	$Cu(NH_3)_4^{2+}$
0.02 M Cu(II) + 4 M NH_4Cl	Fig. 7d	9.5	~240, 620	$Cu(NH_3)_5^{2+}$

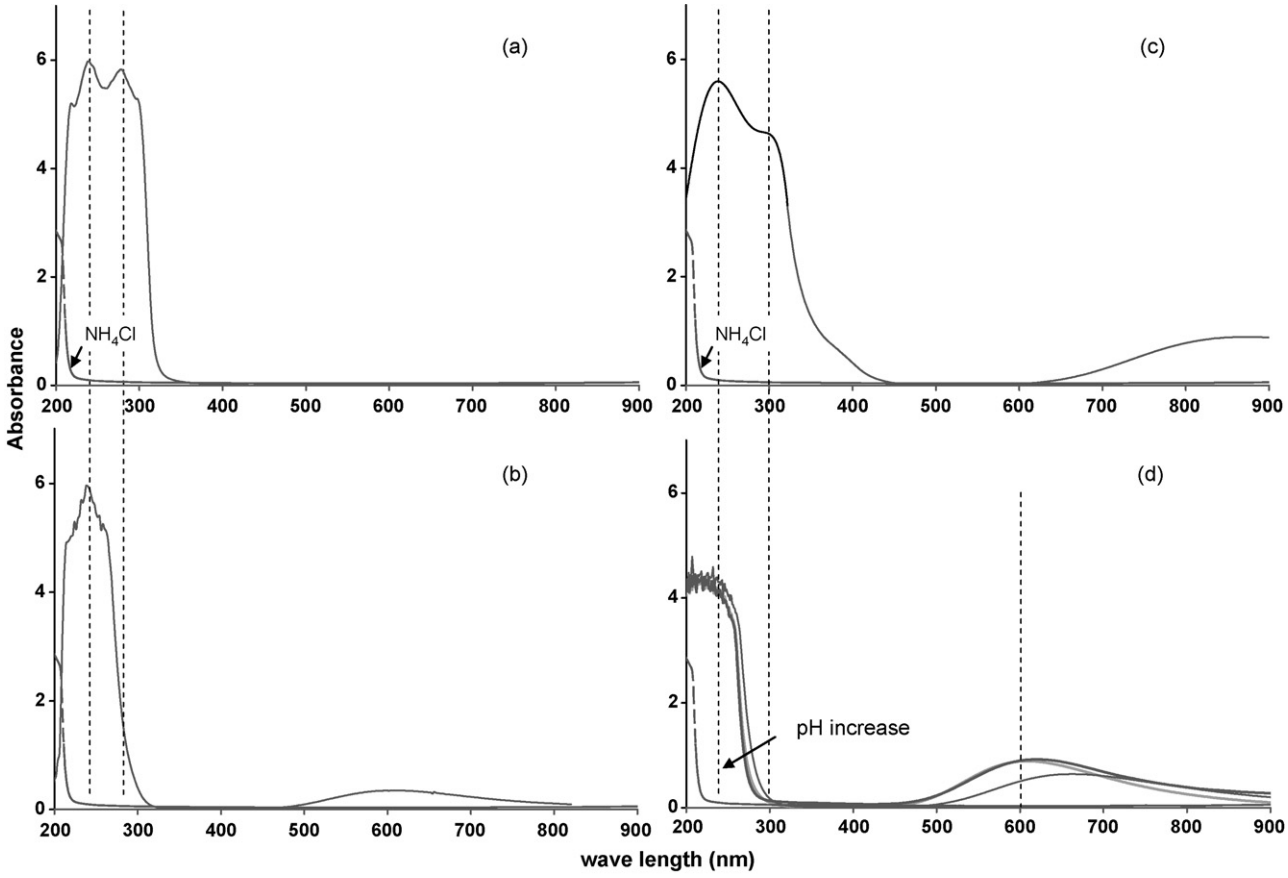

Fig. 6. UV–vis spectra obtained for solutions prepared according to data presented in Table 4.

an absorption band is observed at wavelengths of ca. 600 nm for solution of Cu(I) at pH 9.3. This last attributed to Cu(II) species generated by oxidation of Cu(I) during the experiment (Fig. 6b).

For solutions of Cu(II) at pH 3, where the $CuCl_3^-$ is the predominant specie, the absorption band due to electronic transition between Cu–Cl is also observed (Fig. 6c). In addition, an absorption band around 800 nm is observed. This band is attributed to chloride complexes of copper(II). Fig. 6d shows the UV–vis spectra for solutions of Cu(II) at a pH of 7.4, 8.7 and 9.5. In this figure, it can be observed that the absorption band at ~300 nm disappears, however, a remaining adsorption it is observed, which decreases as the pH increase, being the highest adsorption for the spectrum of pH 7.4, due to the remaining chloride in the complex, $Cu(NH_3)_3Cl^+$. On the other hand, an adsorption band is observed between 500 and 700 nm. The maximum for these absorption bands are located at 660, 605 and 620 nm for pH 7.4, 8.7 and 9.5, respectively. These adsorption bands have been reported for amino complexes of Cu(II) [13,25]. A negative displacement in the adsorption band is expected as the pH increases, due to higher energy of molecules that present absorption at lower wavelength (batochromic effect). This effect is observed for pH 7.4 and 8.5 indicating that $Cu(NH_3)_3Cl^+$ and $Cu(NH_3)_4^{2+}$ are the dominant species for these conditions. However, for pH 9.5 an inverse displacement is observed because the energy of the complex is lowered due to the inclusion of the fifth NH_3 molecule to form the $Cu(NH_3)_5^{2+}$ [26]. It is worth noting that the visible adsorption bands' position (wavelengths), are in agreement with the required energy for the complexes reduction (E_h–pH diagram), which points the stability of the complexes ($CuCl_3^- < Cu(NH_3)_3Cl^+ < Cu(NH_3)_4^{2+} \approx Cu(NH_3)_5^{2+}$). The similitude between the complexes energy between $Cu(NH_3)_4^{2+} \approx Cu(NH_3)_5^{2+}$ is certainly due the coexistence of these complexes at the pH evaluated as it is shown in Fig. 3.

3.2.2. X-ray diffraction analysis

X-ray diffraction (XRD) analysis was used to characterize the solid phases that limit the solubility of copper. Due to the difficulty to generate the necessary amount of Cu(I) precipitates to perform XRD analyses, only Cu(II) species were characterized. The solid phases analyzed were produced following experimental conditions established in the thermodynamic diagrams. Hence, when the pH of the Cu(II) solution was adjusted to a pH between 4.23 and 6.55 a green precipitate was immediately formed. The XRD analysis of this solid is shown in Fig. 7, where it can be observed that the obtained diffraction spectrum fits the pattern of $CuOH_{1.5}Cl_{0.5}$ according to the Joint Committee on Diffraction Standards (JCDS, Fig. 7a) cards [27]. The K_{ps} value ($1 \times 10^{-17.16}$) for $CuOH_{1.5}Cl_{0.5(s)}$, denotes the importance of this species in terms of solubility limitation for Cu(II) at those pH values. As shown in this study (Fig. 4) and as reported by other authors the solubility limitation by $CuOH_{1.5}Cl_{0.5(s)}$ is enhanced when there is high chloride ion concentration [9,18]. However, there are reports showing that for chloride concentrations higher

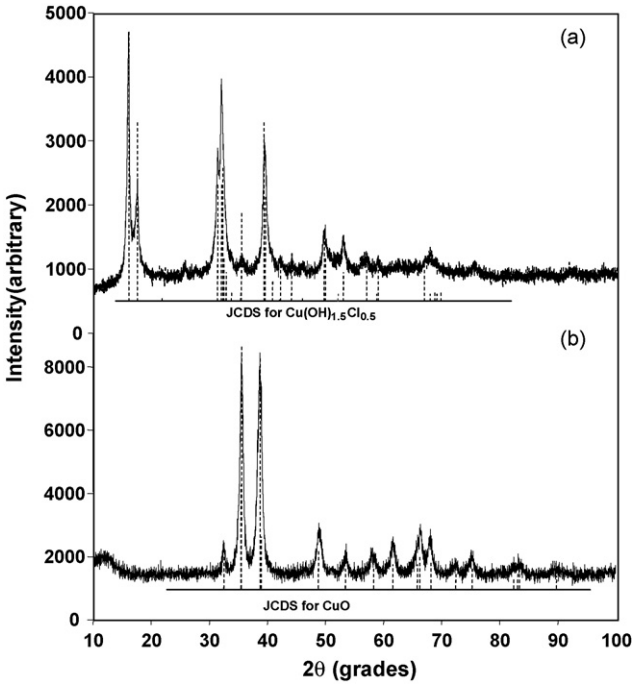

Fig. 7. XRD diagrams obtained for the precipitates: (a) $CuOH_{1.5}Cl_{0.5}$ and (b) CuO. Vertical line groups correspond to the JCPDS card for each solid phase.

than 5.5m the formation of the solid phase $Cu(NH_3)_2Cl_{2(s)}$ is predominant [7]. No indication of those observations has been found at any of the conditions studied in this work. On the other hand, the K_{ps} value for $Cu(NH_3)_2Cl_{2(s)}$ is higher ($1 \times 10^{-1.7}$) than that for $CuOH_{1.5}Cl_{0.5(s)}$.

Another solid phase described in the diagrams for Cu(II) is the $CuO_{(s)}$, in order to generate this precipitate the pH of the solution was risen to a value above 12.5. The XRD spectrum obtained for this solid phase corresponds to a solid with crystallography and chemical composition similar to CuO (Fig. 7b).

3.3. Voltammetric study

A voltammetric study was carried out in order to characterize the electrochemical behavior of Cu(I) and Cu(II) when these ions are present as complexes in a ammonia-chloride medium. The experimental set up was based on results shown by thermodynamic diagrams (Figs. 1–5). The experimental conditions used in this work were chosen on the basis of relating these to hydrometallurgical systems (high chloride and high ammonia concentrations) and they include predominance regions for most of the possible binary and ternary complexes for this medium.

3.3.1. Electrochemistry of the reduction process of Cu(I)

On the basis of the thermodynamic results three pH regions were chosen to characterize the reduction process of Cu(I) complexes in ammonia-chloride medium. Thus, the complexation forms for Cu(I) at the three pH zones (values in parenthesis) were: $CuCl_3^{2-}$ (3) and $Cu(NH_3)_2Cl$ (7.5 and 9.5). The solutions employed in these experiments involved a concentration of 0.02 M Cu(I) which is lower than the used for other experiments as this helped to avoid oxidation to Cu(II). Nevertheless, it was suitable to confirm predictions of existence of all complexes under study.

Cyclic voltammograms (CV) obtained for each solution employed are illustrated in Fig. 8. In all CV's it is observed that the open circuit potential (OCP) in all solutions is within the potential region of equilibrium for the Cu(I) complexes, and it follows the same trend depicted by E_h–pH diagrams, that is, a negative displacement as the pH increases. Given the difficulty of stabilizing Cu(I), it was not unexpected to observe the presence of some Cu(II) in the solutions employed (initial reduction wave in Fig. 8b and c), fortunately the amount seems to be minimal, thus the processes observed account for those of Cu(I) complexes unless otherwise stated. Therefore the initial Cu(II) would not significantly contribute to the peak labeled as Ic', that corresponds to reduction of Cu(I) to Cu(0). Thus, the reactions proposed for each pH value would be:

$$\text{pH}\quad 3\quad CuCl_3^{2-}(aq) + e^- = Cu(s)$$

$$\text{pH}\quad 7.5\quad Cu(NH_3)_2Cl(aq) + H^+(aq) + e^- = Cu(s) + NH_4^+(aq) + NH_3(aq) + Cl^-(aq)$$

$$\text{pH}\quad 9.5\quad Cu(NH_3)_2Cl(aq) + e^- = Cu(s) + 2NH_3(aq) + Cl^-(aq)$$

It can be devised from these equations that for alkaline pH there would be an excess of ammonia at the interface, which seems to promote dissolution of Cu(0), this observed as a small wave (Ia′) before peak IIa′ develops. As soon as the excess of ammonia is consumed the expected process of Cu(0) oxidation to Cu(I) is observed. Thus, peak IIa′ in each voltammogram of Fig. 8, would correspond to oxidation of Cu(0) to $Cu(NH_3)_2Cl$ for pH 7.5 and 9.5 (Fig. 8b and c) and oxidation of Cu(0) to $CuCl_3^{2-}$ at pH 3 (Fig. 8a). In correspondence with thermodynamic predictions it is observed that there is a higher overpotential involved for oxidation of Cu(0) at lower pH, it however, seems to be a process kinetically favored.

3.3.2. Electrochemistry of the oxidation process of Cu(I)

Solutions such as the ones described above were used to characterize the oxidation behavior of Cu(I) complexes and the corresponding cyclic voltammograms are illustrated in Fig. 9. In this case, the redox couples involved include the pH zone around 8.73 and a CV for this pH region is included. In all cases a non-reversible redox behavior is observed for the Cu(I)/Cu(II) complexes pairs, which present a $\Delta E_p >> 0.059$ V. Thus, it is proposed that for each pH zone studied the reactions involved are:

$$\text{pH}\quad 3\quad CuCl_3^{2-}(aq) \rightarrow CuCl_3^-(aq) + e^-$$

$$Cu(NH_3)_2Cl(aq) + (x-2)NH_4^+(aq) \rightarrow Cu(NH_3)_xCl_y^{(2-y)+}(aq) + (x-2)H^+(aq) + (1-y)Cl^-(aq) + e^-$$

where pH 7.5 ($x=3$, $y=1$), pH 8.73 ($x=4$, $y=0$) and pH 9.5 ($x=5$, $y=0$).

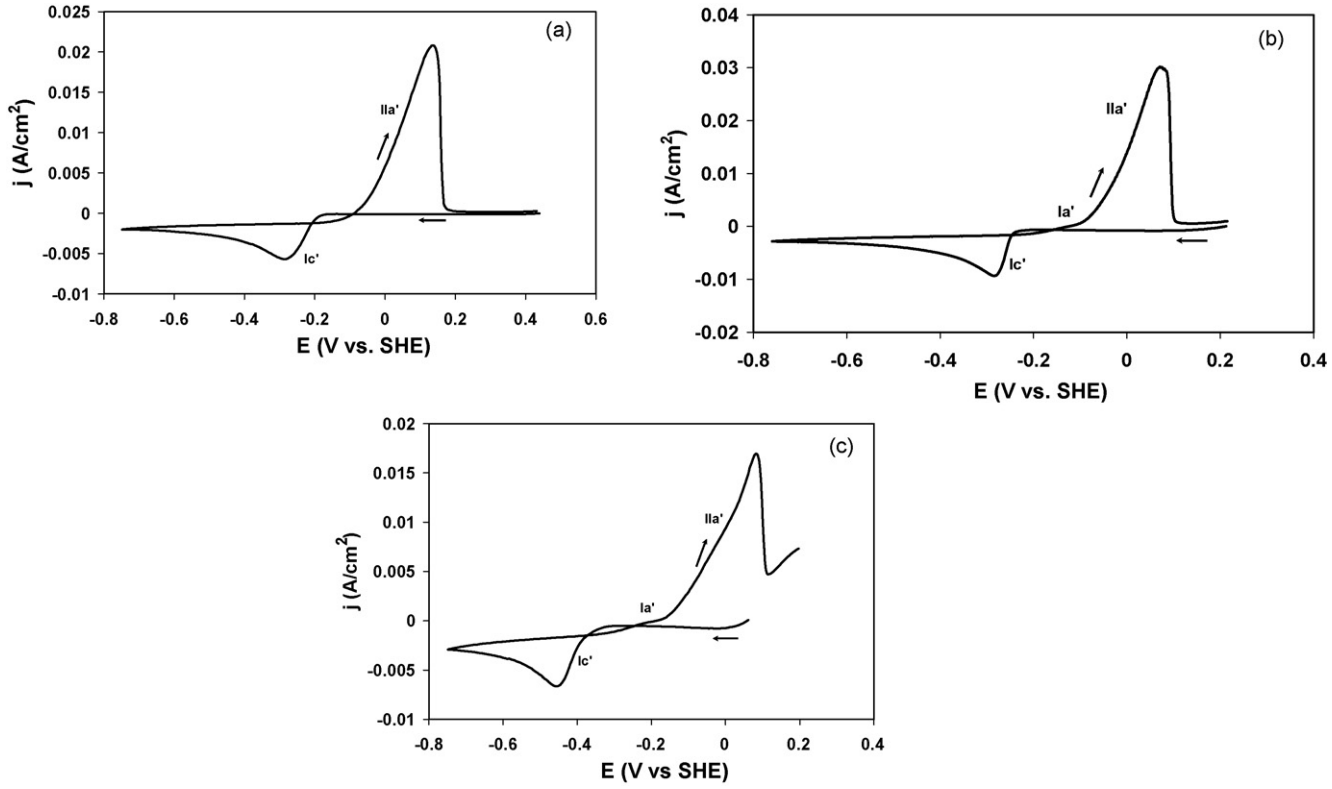

Fig. 8. Voltammetric response of Cu(I) complexes on a glassy carbon electrode at 25 °C, scan rate of 100 mV s^{-1}. The scan was initiated from the OCP towards the negative direction. All solutions employed containing 0.02 M CuCl and 4 M NH_4Cl and adjusted at different pH values: (a) 3.0, (b) 7.5 and (c) 9.5.

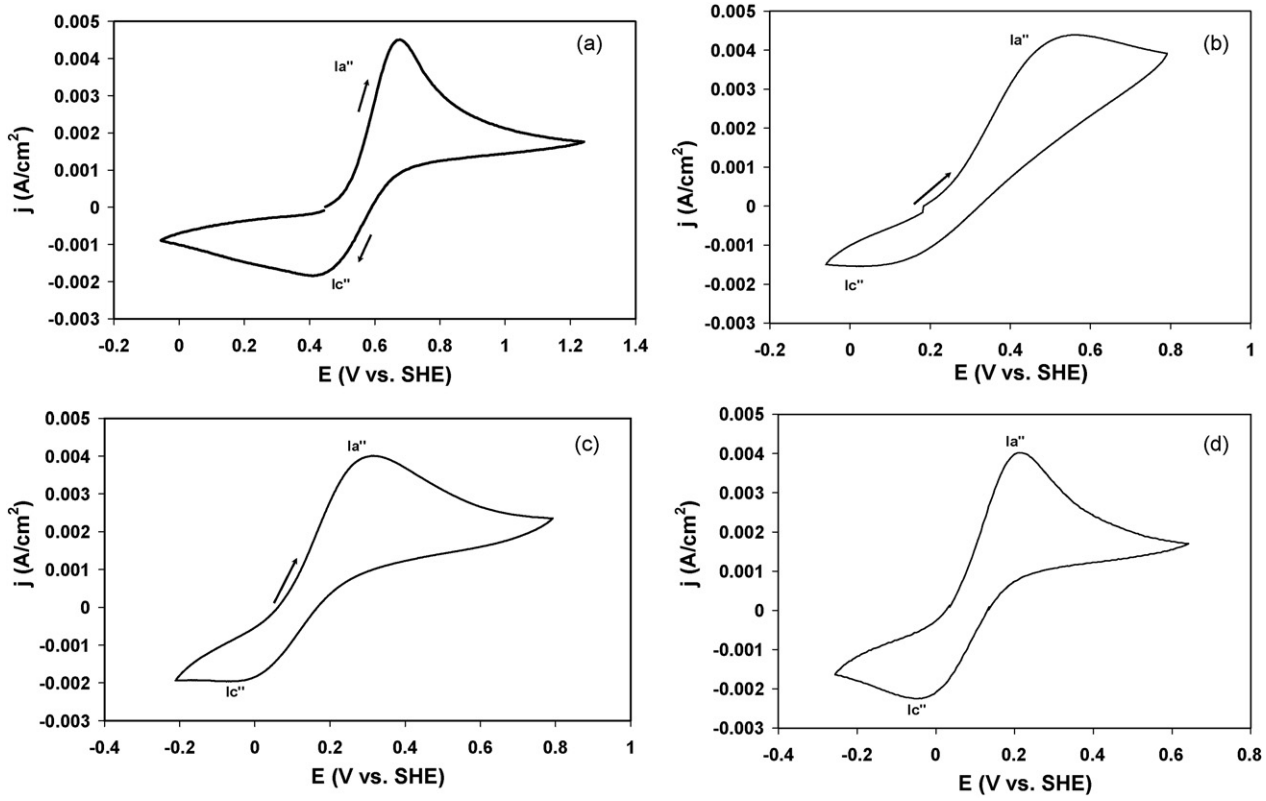

Fig. 9. Voltammetric response of Cu(I) complexes on a glassy carbon electrode at 25 °C, scan rate of 100 mV s^{-1}. The scan was initiated from the OCP towards the positive direction. All solutions employed containing 0.02 M CuCl and 4 M NH_4Cl and adjusted at different pH values: (a) 3.0 and (b) 9.5.

3.3.3. Electrochemistry of the reduction process of Cu(II)

To characterize the electrochemical reduction of Cu(II), four pH zones were chosen. These zones were chosen on the basis of the species that are predicted to be predominant at those pH values (values in parenthesis), that is: $CuCl_3^-$ (3), $Cu(NH_3)_3Cl^+$ (7.5), $Cu(NH_3)_4^{2+}$ (8.73) and $Cu(NH_3)_5^{2+}$ (9.3).

Cyclic voltammograms (CV) were obtained in solutions of 0.2 M Cu(II) + 4 M NH_4Cl, which were adjusted at the pH values mentioned above and the results are illustrated in Fig. 10. It is observed that the open circuit potential for each CV shifts towards negative values as the pH increases and that it follows the same trend observed in the E_h–pH diagram (Fig. 5). All CV's show two cathodic processes labeled as Ic and IIc on the direct scan and depending on pH several anodic processes labeled as Ia, IIa and IIIa on the reverse scan.

Except for $CuCl_3^-$ (Fig. 10a), it is proposed that in all cases Ic corresponds to the reduction of the Cu(II) complex to $Cu(NH_3)_2Cl$, according to

$$Cu(NH_3)_xCl_y^{(2-y)+}(aq) + (x-2)H^+(aq) + (1-y)Cl^-(aq) + e^- = Cu(NH_3)_2Cl(aq) + (x-2)NH_4^+(aq)$$

where pH 7.5 ($x=3$, $y=1$), pH 8.73 ($x=4$, $y=0$) and pH 9.5 ($x=5$, $y=0$).

Thus, in the case of $CuCl_3^-$ the reduction process would be

$$CuCl_3^-(aq) + e^- = CuCl_3^{2-}(aq)$$

As expected in all cases the peak current for process Ic is practically the same, as in all cases a one electron process is involved and the displacement in peak potential as predicted it is a function of the change in sphere coordination.

Thus, IIc in Fig. 10b–d corresponds to the reduction of $Cu(NH_3)_2Cl$ to metallic copper and for Fig. 10a reduction of $CuCl_3^{2-}$ to metallic copper, according to the following reactions:

$$Cu(NH_3)_2Cl(aq) + 2H^+(aq) + e = Cu(s) + NH_4^+(aq) + NH_3(aq) + Cl^-(aq)$$

$$CuCl_3^{2-}(aq) + e = Cu(s) + 3Cl^-(aq)$$

Different from experiments of direct reduction of Cu(I) complexes to Cu metal, the corresponding potential for peak IIc (Fig. 10) is more negative than the potential for peak Ic′ (Fig. 8),

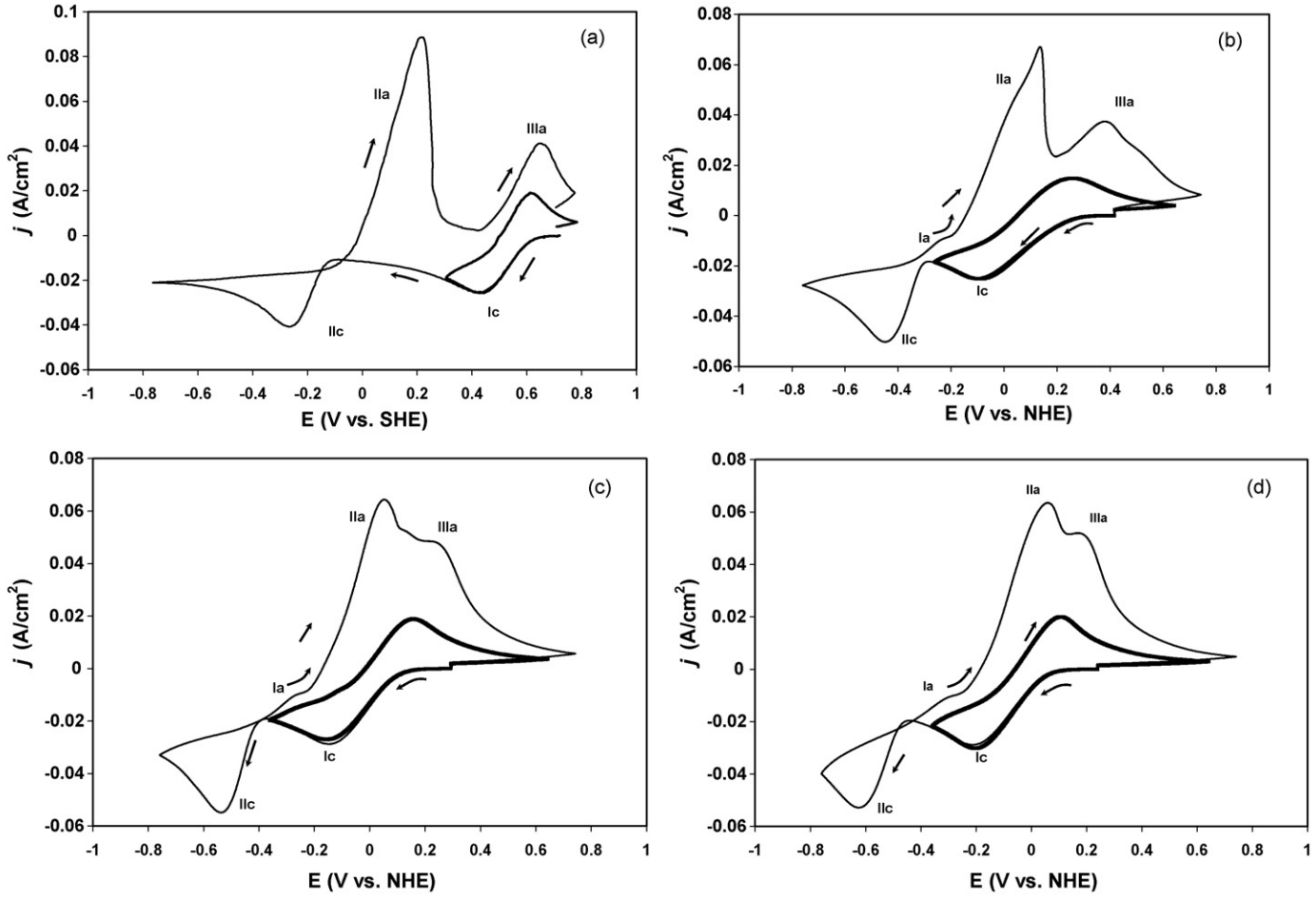

Fig. 10. Voltammetric response of Cu(II) complexes on a glassy carbon electrode at 25 °C, scan rate of 100 mV s^{-1}. The scan was initiated from the OCP towards the negative direction. Thick line corresponds to voltammetric response obtained when potential was switched before reduction of Cu(I) to Cu(0). All solutions employed containing 0.2 M $CuCl_2$ and 4 M NH_4Cl and adjusted at different pH values: (a) 3.0, (b) 7.5, (c) 8.73 and (d) 9.5.

Table 5
Experimental and theoretical potentials calculated for Cu(II)/Cu(I) couples in ammonia-chloride system

pH	Redox couple	$E^{\circ\prime}_{\text{Thermo.}}$ (V)	$E^{\circ\prime}_{\text{exp.}}$ [a] (V)	$E^{\circ\prime}_{\text{exp.}}$ [b] (V)	$\lvert E^{\circ\prime}_{\text{Thermo.}} - E^{\circ\prime}_{\text{exp.}}\rvert$ (V)	
3	$CuCl_3^-/CuCl_3^{2-}$	0.495	0.542	0.499	0.047	0.004
7.5	$Cu(NH_3)_3Cl^+/Cu(NH_3)_2Cl$	0.212	0.104	0.245	0.108	0.033
8.73	$Cu(NH_3)_4^{2+}/Cu(NH_3)_2Cl$	0.104	0.020	0.117	0.084	0.013
9.3	$Cu(NH_3)_5^{2+}/Cu(NH_3)_2Cl$	0.036	−0.029	0.057	0.065	0.021

[a] From Cu(II)–NH_3–Cl^- system, Fig. 10.
[b] From Cu(I)–NH_3–Cl^- system, Fig. 9.

this as a result of having a higher concentration of Cu(I) complexes in this case.

As the sweep is reversed a similar behavior to that observed for oxidation of Cu(0) formed from Cu(I) solutions at alkaline pH (Fig. 8b–d) is observed, which as previously suggested could be triggered by the excess of ammonia at the interface. Therefore, the same oxidation product is obtained for peak IIa, $Cu(NH_3)_2Cl$. The interface at this point would be the same for the three alkaline systems (pH 7.5, 8.73, 9.5), however, as indicated by the E_h–pH diagram the subsequent oxidation to Cu(II) requires a lower overpotential for the change of $Cu(NH_3)_2Cl$ to either $Cu(NH_3)_5^{2+}$ or $Cu(NH_3)_4^{2+}$; hence, the potential difference between peaks IIa and IIIa is lower as compared to the oxidation to $Cu(NH_3)_3Cl^+$ (Fig. 10c and d). For the acidic zone, a completely different oxidation behavior is observed and sharper anodic peaks depicting oxidation of Cu(0) to $CuCl_3^{2-}$ (peak IIa) and subsequent oxidation to $CuCl_3^-$ (peak IIIa) are obtained. The oxidation of the predominant species for each species at each pH zone studied (peak IIIa) was corroborated by the direct oxidation from Cu(I) to Cu(II) species (CV's at a negative switching potential before reduction of Cu(I) to Cu(0)).

3.3.4. Thermodynamic calculations from experimental data

Formal potentials ($E^{\circ\prime}$) for all Cu(I)/Cu(II) couples involved in voltammograms of Figs. 9 and 10 were determined using conventional electrochemical methods [28]. These values were then compared against the thermodynamic values ($E^{\circ\prime}_{\text{Thermo}}$) calculated for the E_h–pH diagram. The comparative analysis (Table 5) shows than in both systems there is a higher deviation ($E^{\circ\prime}_{\text{Thermo}} - E^{\circ\prime}$) when the pH approaches the neutral zone, it, however, is larger for the data obtained with results of reduction of Cu(II) to Cu(I) (Fig. 10) than the obtained from results of oxidation of Cu(I) to Cu(II) (Fig. 9). All of this could be associated to the fact that the Cu(II) system involves a wider mixture of complexes throughout the whole pH range and this is notably marked around the neutral zone. Therefore, such results suggest that the coexistence of multiple complexes affects the reversibility of the redox processes of the predominant species.

Likewise, formal potentials for the Cu(I)/Cu(0) system were established (Table 6), however, different from the Cu(I)/Cu(II) system, in this case crossover potentials (E_{cross}) values were used instead, since as it has been found E_{cross} corresponds to the reversible potential of the metal redox couple deposited with the ion in solution [20,29]. From data in Table 7, it can be observed that except for pH 3, which shows a high deviation

Table 6
Experimental and theoretical potentials calculated for Cu(I)/Cu(0) couples in ammonia-chloride system

pH	Redox couple	$E_{\text{cross.}}$ (V)	$E^{\circ\prime}_{\text{Thermo.}}$ (V)	$\lvert E^{\circ\prime}_{\text{Thermo.}} - E^{\circ\prime}_{\text{exp.}}\rvert$ (V)
3	$CuCl_3^{2-}/Cu$	−0.092	0.018	0.110
7.5	$Cu(NH_3)_2Cl/Cu$	−0.112	−0.073	0.039
9.3	$Cu(NH_3)_2Cl/Cu$	−0.246	−0.286	0.040

Table 7
Formation constants for binary and ternary Cu(I) and Cu(II) complexes in ammonia-chloride medium

Reaction	$\log \beta$	$\log \beta$[a]
$Cu^+ + 3Cl^- \leftrightarrow CuCl_3^{2-}$	5.99 [19]	6.05
$Cu^{2+} + 3Cl^- \leftrightarrow CuCl_3^-$	−0.3 [5]	−0.28
$Cu^+ + 2NH_3 + Cl^- \rightarrow Cu(NH_3)_2Cl$	11.3 [8]	11.55
$Cu^{2+} + Cl^- + 3NH_3 \rightarrow Cu(NH_3)_3Cl^+$	11.73 [5]	11.34

[a] This work.

($E_{\text{cross}} - E^{\circ\prime}_{\text{Thermo}}$), there is good agreement with theoretical data. The deviation for acid pH is attributed to a lower stability of the binary complexes, which require a higher energy for charge transfer as compared to the ternary complexes. Therefore, this deviation could be considered a deviation from reversibility for pH 3.

Finally, supported on these last results and using reported data (E and β) for well known systems (i.e. $Cu(NH)_4^{2+}$, $Cu(NH_3)_5^{2+}$), formation constants (β) for some of the binary and ternary complexes were calculated (Table 7). Comparison of these results against data reported in the literature (Tables 1 and 3) shows a good agreement, which further supports the predictions made for conditions typical of hydrometallurgical systems.

4. Conclusions

An electrochemical characterization has been performed and it has been shown the redox characteristics of several binary and ternary copper complexes. In general ternary complexes are shown to be more stable and this has been particularly evident for the Cu(I) system. The existence of the proposed complexes for each pH region studied has been supported by calculations of formation constants. The results show a general agreement with respect to thermodynamic predictions and the deviations observed in some cases are attributed to the kinetic effect

provoked by ammonia excess at the interface. These results together with UV–vis and XRD spectra allowed to confirm the existence of copper species normally not considered.

The inclusion of ternary complexes in this study allowed a better understanding of Cu(I) and Cu(II) solubility in ammonia-chloride media. Thus, it has been shown the importance of considering the combined effect of ammonia and chloride concentration on the stability of the different copper complexes. In this way and for the experimental conditions studied, it has been found that the only solubility limitation for Cu(I) is the formation of Cu_2O at alkaline pH values, however, this limitation is notably reduced if the copper ternary complex $Cu(NH_3)_2Cl$ is formed. Although, Cu(II) presents solubility limitations either for formation of $Cu(OH)_{1.5}Cl_{0.5}$ under acidic conditions, and because of CuO formation at very alkaline pH. It has been highlighted that for close to neutral pH the solubility limitation is reduced by $Cu(NH_3)_3Cl^+$ formation.

The results here presented, further support the potential application of this medium in copper hydrometallurgical processes.

Acknowledgements

Financial support for this study has been obtained through CONACyT grant 39585-Y and UASLP-C03-FRC-06-5.6. J. Vázquez is indebted for the scholarship provided by CONACyT to carry out M.Eng. studies. An especial acknowledgement to the reviewers who made comments and suggestions that notably improved this paper.

References

[1] E. Peters, Hydrometallurgy 29 (1992) 431.
[2] G.M. Swinkels, R.M. Berezowsky, CIM Bull. 71 (1978) 105.
[3] R. Winand, Hydrometallurgy 27 (1981) 285.
[4] C. Ek, J. Frenay, J.C. Herman, Hydrometallurgy 8 (1982) 17.
[5] J.L. Limpo, J.M. Figueiredo, S.L. Amer, Hydrometallurgy 28 (1992) 149.
[6] M. Olper, in: G.W. Warren (Ed.), EPD Congress, The Minerals, Metals and Materials Society, 1994, p. 513.
[7] J.L. Limpo, A. Luis, M.C. Cristina, Rev. Metal. Madrid 29 (1993) 27.
[8] J.S. Solis, G. Hefter, P.M. May, Aust. J. Chem 48 (1995) 1283.
[9] C. Nila, I. González, Hidrometallurgy 47 (1996) 63.
[10] D. Grujicic, B. Pesic, Electrochim. Acta 50, 22 (2005) 4426.
[11] J. Crousier, I. Bimaghra, Electrochim. Acta 34, 8 (1989) 1205.
[12] J. Black, L. Spiccia, D.C. McPhail, in: C. Young, A. Alfantzi, C. Anderson, A. James, D. Dreisinger, B. Harris (Eds.), Proceedings of the 5th International symposium of hydrometallurgy, vol. x, Vancouver, Canada, 1990, p. 183.
[13] A. Lam, D.B. Dreisinger, in: C. Young, A. Alfantzi, C. Anderson, A. James, D. Dreisinger, B. Harris (Eds.), Proceedings of the 5th International Symposium of Hydrometallurgy, Vancouver, Canada, 2003, p. 195.
[14] G. Eriksson, Anal. Chim. Acta 112 (1979) 375.
[15] I. Puigdomenech, INPUT, SED, and PREDOM: Computer programs, drawing equilibrium diagrams, TRITA-OOK-3010, Royal Institute of Technology, September 1983, 12 pp.
[16] National Institute of Standards and Technology, NIST, Critically Selected Stability Cosntants of Metal Complexes, 2001.
[17] G.W. McDonald, A. Saud, M.S. Barger, J.A. Koutski, S.H. Langer, Hydrometallurgy 18 (1987) 321.
[18] R.M. Smith, A.E. Martell, Critical Stability Constants, vol. 4, Plenum Press, New York, 1976.
[19] M. Wang, Y. Zhang, M. Muhammed, Hydrometallurgy 45 (1997) 53.
[20] D.M. Muir, In: E. Peek, G. Van Weert (Eds.), Chloride Metallurgy, vol. II, 32nd Annual Hydrometallurgy Meeting, 2002, p. 759.
[21] C. Nila, I. González, J. Electroanal. Chem. 401 (1996) 171.
[22] Z.D. Stankovic, Electrochim. Acta 29 (1984) 407.
[23] I.V. Gorbunova, L.I. Lyamina, K.M. Gorbunova, Sov. Electrochem. 23 (1987) 1027.
[24] A. Ramos, M. Miranda, I. Gonzalez, J. Electrochem. Soc. 148 (2001) C315.
[25] M. Valli, S. Matsuo, H. Wakita, T. Yamaguchi, M. Nombra, Inorg. Chem. 35 (1996) 5642.
[26] F. Cotton, G. Wilkinson, Advanced Inorganic Chemistry, Interscience Publishers–Wiley, USA, 1990.
[27] JCDS-International Centre for Diffraction Data, Ref: Swanson, Tatge, Natl. Bur Stand (U.S), Circ., vol. 539, no. I, 1953, p. 49.
[28] A. Bard, L.R. Faulkner, Electrochemical Methods: Fundamentals and Applications, Wiley and Sons, USA, 1980.
[29] S. Flecther, C.S. Halliday, D. Gates, M. Westcott, T. Lwin, G. Nelson, J. Electroanal. Chem. 159, 267 (1983).